Journal of Coordination Chemistry
Publication details, including instructions for authors and subscription information:
http://www.tandfonline.com/loi/gcoo20

Homo- and heterometallic complexes based on polytopic carboxylic acid: synthesis, characterization, and property

Ming-Li Liu [a], Yu-Xia Wang [b], Wei Shi [b] & Jian-Zhong Cui [a c]

[a] Department of Chemistry, Tianjin University, Tianjin 300072, P.R. China

[b] Department of Chemistry, Nankai University, Tianjin 300071, P.R. China

[c] Key Laboratory of Advanced Energy Materials Chemistry (Ministry of Education), Nankai University, Tianjin 300071, P.R. China

Published online: 14 May 2012.

To cite this article: Ming-Li Liu, Yu-Xia Wang, Wei Shi & Jian-Zhong Cui (2012) Homo- and heterometallic complexes based on polytopic carboxylic acid: synthesis, characterization, and property, Journal of Coordination Chemistry, 65:11, 1915-1925, DOI: 10.1080/00958972.2012.684382

To link to this article: http://dx.doi.org/10.1080/00958972.2012.684382

Journal of Coordination Chemistry
Vol. 65, No. 11, 10 June 2012, 1915–1925

Homo- and heterometallic complexes based on polytopic carboxylic acid: synthesis, characterization, and property

MING-LI LIU†, YU-XIA WANG‡, WEI SHI‡ and JIAN-ZHONG CUI*†§

†Department of Chemistry, Tianjin University, Tianjin 300072, P.R. China
‡Department of Chemistry, Nankai University, Tianjin 300071, P.R. China
§Key Laboratory of Advanced Energy Materials Chemistry (Ministry of Education), Nankai University, Tianjin 300071, P.R. China

(*Received 27 September 2011; in final form 9 January 2012*)

Two heterometallic $[K_4M_4(HL)_4(H_2O)_{12}]$ (M=Co (**1**), Ni (**2**)) and two homometallic $[M_2L(H_2O)_7]\cdot 2H_2O$ ((M=Co (**3**), Ni (**4**)) (H_4L = (2-(bis(carboxymethyl)amino) terephthalic acid) have been synthesized and characterized by elemental analysis, FT-IR spectrum, and single-crystal X-ray diffraction. The isomorphous **1** and **2** contain K^+ and M^{2+}, in which K^+ were bridged with M^{2+} through μ-HL^{3-} and μ-H_2O, leading to 2-D layer structures. The isomorphous **3** and **4** show homometallic binuclear complexes with μ-HL^{3-} as the bridging ligand. Various H-bonds including different H-bond helical chains form, by which **3** and **4** assemble into 3-D supramolecular frameworks. TG analysis indicates that the decomposition temperatures are $[K_4M_4(HL)_4(H_2O)_{12}]$ (**1**) > $[M_2L(H_2O)_7]\cdot 2H_2O$ (**3**) > H_4L.

Keywords: Supramolecular framework; Helical chains; Cobalt complex; Nickel complex

1. Introduction

Design and synthesis of organic–inorganic hybrid complexes have attracted significant interest for intriguing topologies and applications in non-linear optics, luminescence, magnetism, etc. [1, 2]. Recent research focused on complexes with multidentate ligands such as polycarboxylic acids [3–5]. With two or more coordinated groups, polytopic ligands can be applied to build intriguing molecular architectures with special magnetism, and optical properties due to their variety of binding or bridging. Magnetic and adsorption materials based on them can be documented [6, 7]. Recently, 2-(bis(carboxymethyl)amino) terephthalic acid (H_4L) as a ligand has been employed in the preparation of metal–organic complexes. H_4L contains four carboxylic acids in a tripod. Due to various coordination modes of carboxylic acid and strong chelation of the tripod ligand, H_4L should be a good ligand in constructing multinuclear complexes and even supramolecular frameworks. Two copper complexes with alternating magnetic coupling have been obtained and reported [8], confirming our anticipation. An interesting phenomenon has been found in cobalt and nickel complexes. Alkali metal

*Corresponding author. Email: cuijianzhong@tju.edu.cn

ISSN 0095-8972 print/ISSN 1029-0389 online
http://dx.doi.org/10.1080/00958972.2012.684382

ions usually have high coordination numbers and are employed as template agents in cyclic organic compounds [9, 10] or host-guest chemistry [11], and are rarely used in assembling metal–organic complexes. In our synthesis, introduction of potassium ions leads to 2-D heterometallic complexes $[K_4M_4(HL)_4(H_2O)_{12}]$ (M=Co (**1**), Ni (**2**)), which can be described as a template synthesis. The absence of potassium ions resulted in only homometallic binuclear complexes $[M_2L(H_2O)_7]\cdot 2H_2O$ ((M=Co (**3**), Ni (**4**)), confirming the template roles played in **1** and **2**. Syntheses, structures, and thermal properties are discussed in the following text.

2. Experimental

2.1. *Materials and characterization*

2-(Bis(carboxymethyl)amino)terephthalic acid (H_4L) was prepared as reported [12]. All other reagents were commercial and used without purification. The synthesis routes of **1**–**4** are shown in scheme 1.

Elemental analyses for C, H, and N were carried out with a Vario EL III elemental analyzer. Infrared (IR) spectra were taken with a Bruker tensor 27 FTIR spectrophotometer from 4000 to 400 cm^{-1} using KBr pellets. Thermogravimetric analyses were studied by a Delta Series TA-SDT Q600 in nitrogen using Al crucibles.

2.2. *Synthesis*

2.2.1. Synthesis of $[K_4Co_4(HL)_4(H_2O)_{12}]$ (1). A solution of $Co(OAc)_2\cdot 4H_2O$ (63.2 mg, 0.35 mmol) in 5 mL methanol was added to a stirred solution of H_4L (60.3 mg, 0.20 mmol) in 5 mL methanol. Ten minutes later, solid KOH (11.2 mg, 0.20 mmol) and four drops of KNO_3 (0.20 mol L^{-1}) were sequentially added to the mixture. The resulting solution was filtered after stirring for 30 min. Red block crystals were isolated

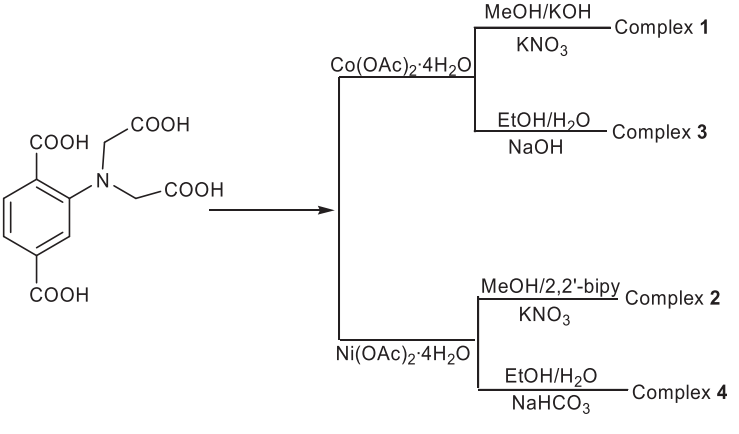

Scheme 1. Synthesis routes of **1**–**4**.

from the filtrate after standing for 3 weeks with the yield of 34%. Anal. Calcd for $C_{12}H_8CoKNO_{11}$ (%): C, 32.71; H, 1.81; N, 2.49. Found (%): C, 32.54; H, 2.01; N, 2.66.

2.2.2. Synthesis of $[K_4Ni_4(HL)_4(H_2O)_{12}]$ (2). A solution of $Ni(OAc)_2 \cdot 4H_2O$ (62.1 mg, 0.35 mmol) in 5 mL methanol was added to the solution of H_4L (62.3 mg, 0.20 mmol) in 5 mL methanol under stirring. Green precipitate slowly formed from the reaction, to which 2,2′-bipyridine (311.8 mg, 2.0 mmol) and four drops of KNO_3 (0.20 mol L^{-1}) were added. The mixture was filtered after reacting for 1 h. Cyan block crystals were obtained after leaving the filtrate for 1 month. The yield is 27%. Anal. Calcd for $C_{12}H_{14}NiKNO_{11}$ (%): C, 32.28; H, 3.14; N, 3.17. Found (%): C, 32.33; H, 3.41; N, 3.32.

2.2.3. Synthesis of $[Co_2L(H_2O)_7] \cdot 2H_2O$ (3). $Co(OAc)_2 \cdot 4H_2O$ (179.3 mg, 1.00 mmol) in a 15 mL mixture of EtOH/H_2O (V/V = 1/1) was added to a stirred solution of 15 mL EtOH/H_2O (V/V = 1/1) containing H_4L (276.9 mg, 1.00 mmol) and NaOH (80.4 mg, 2.00 mmol). The resulted mixture was filtered after 3 h. Red block crystals were isolated from the filtrate after leaving undisturbed for 3 weeks and dried in air. The yield is 85 mg (30% based on Co atoms). Anal. Calcd for $C_{12}H_{25}Co_2NO_{17}$ (%): C, 25.12; H, 4.36; N, 2.44. Found (%): C, 25.44; H, 4.67; N, 2.32.

2.2.4. Synthesis of $[Ni_2L(H_2O)_7] \cdot 2H_2O$ (4). Complex **4** was synthesized in the similar procedure as **3** except changing $Co(OAc)_2 \cdot 4H_2O$ and NaOH for $Ni(OAc)_2 \cdot 4H_2O$ and $NaHCO_3$. The yield is 42%. Anal. Calcd for $C_{12}H_{25}NNi_2O_{17}$ (%): C, 25.14; H, 4.36; N, 2.44. Found (%): C, 25.32; H, 4.53; N, 2.26.

2.3. *Single-crystal X-ray structure determination*

Single crystals of **1**–**4** with suitable dimensions were mounted onto thin glass fibers; intensity data were collected at 294 K on a Bruker SMART 1000-CCD diffractometer (Mo-Kα radiation, $\lambda = 0.71073$ Å) in ω scan modes. Structures were solved by the direct method followed by difference Fourier syntheses and then refined by full-matrix least-square refinement on F^2 using SHELXTL [13, 14]. All non-hydrogen atoms were refined with anisotropic parameters while hydrogen atoms were placed in calculated positions and refined using a riding model. All crystallographic data are listed in table 1.

3. Results and discussion

3.1. *Synthesis and FT-IR spectroscopy*

The four complexes were prepared at room temperature with different solvent and alkali metal leading to different hetero- and homometallic complexes. For **1** and **2**, methanol, KOH or 2,2′-bipyridine, and extra KNO_3 were used, which favored the formation of heterometallic complexes **1** and **2**. To compare with **1** and **2**, KNO_3 was replaced by $NaNO_3$ in the above synthesis and no similar structure was obtained. Obviously, the extra K^+ acts as template in building the heterometallic framework.

Table 1. Crystallographic data and structural refinement details for **1–4**.

Complex	**1**	**2**	**3**	**4**
Empirical formula	$C_{12}H_{14}CoKNO_{11}$	$C_{12}H_{14}KNiNO_{11}$	$C_{12}H_{25}Co_2NO_{17}$	$C_{12}H_{25}NNi_2O_{17}$
Formula weight	446.27	446.05	573.19	572.75
Temperature (K)	294(2)	293(2)	293(2)	293(2)
Crystal system	Monoclinic	Monoclinic	Monoclinic	Monoclinic
Space group	$C2/c$	$C2/c$	$P2_1/n$	$P2_1/n$
Unit cell dimensions (Å, °)				
a	30.763(4)	30.549(6)	13.108(3)	13.021(3)
b	7.9210(10)	7.8298(16)	7.7136(15)	7.6576(15)
c	13.5220(17)	13.459(3)	21.615(4)	21.482(4)
α	90	90	90	90
β	93.105(2)	93.47(3)	105.70(3)	105.77(3)
γ	90	90	90	90
Volume (Å^3), Z	3290.1(7), 8	3213.4(11), 8	2104.0(7), 4	2061.4(7), 4
Calculated density (g cm^{-3})	1.802	1.844	1.810	1.845
Absorption coefficient (mm^{-1})	1.358	1.530	1.663	1.914
θ range for data collection (°)	2.65–25.02	2.67–25.02	1.96–25.02	1.97–25.02
Limiting indices	$-30 \le h \le 36$; $-8 \le k \le 9$; $-11 \le l \le 16$	$-36 \le h \le 36$; $-9 \le k \le 9$; $-16 \le l \le 16$	$-14 \le h \le 15$; $-9 \le k \le 9$; $-25 \le l \le 21$	$-14 \le h \le 15$; $-9 \le k \le 9$; $-23 \le l \le 25$
Reflections collected	8225	15,823	13,620	13,224
Independent reflection	2901 [R(int) = 0.0264]	2844 [R(int) = 0.0365]	3710 [R(int) = 0.0329]	3621 [R(int) = 0.0401]
Data/restraints/parameters	2901/0/260	2844/0/260	3710/0/340	3621/3/340
Goodness-of-fit on F^2	1.041	1.063	1.037	1.028
Final R indices [$I > 2\sigma(I)$]	$R_1 = 0.0247$, $wR_2 = 0.0586$	$R_1 = 0.0273$, $wR_2 = 0.0650$	$R_1 = 0.0236$, $wR_2 = 0.0605$	$R_1 = 0.0288$, $wR_2 = 0.0866$
R indices (all data)	$R_1 = 0.0323$, $wR_2 = 0.0619$	$R_1 = 0.0282$, $wR_2 = 0.0656$	$R_1 = 0.0266$, $wR_2 = 0.0624$	$R_1 = 0.0324$, $wR_2 = 0.0885$
Largest difference peak and hole (e Å^{-3})	0.363 and −0.246	0.303 and −0.323	0.379 and −0.383	0.423 and −0.681

Table 2. Important bond lengths (Å) and angles (°) of **1** and **2**.

1			
Co(1)–O(1)	2.0130(15)	K(1)–O(8)	2.8601(16)
Co(1)–O(5)	2.0244(15)	K(1)–O(11)	2.863(2)
Co(1)–O(9)	2.0644(18)	K(1)–O(1)$^{\#1}$	2.9213(18)
Co(1)–O(7)	2.0749(15)	K(1)–O(7)	2.9344(15)
Co(1)–O(10)	2.1049(16)	K(1)–O(10)$^{\#1}$	2.9522(17)
Co(1)–N(1)	2.1666(17)	K(1)–O(6)$^{\#2}$	3.0696(17)
Co(1)–K(1)$^{\#1}$	3.6199(6)	K(1)–O(9)$^{\#1}$	3.179(2)
K(1)–O(5)$^{\#2}$	2.7473(15)	K(1)–O(11)$^{\#4}$	3.202(2)
K(1)–O(8)$^{\#3}$	2.7941(16)	O(9)–Co(1)–O(7)	177.73(7)
O(1)–Co(1)–O(5)	170.80(7)	O(10)–Co(1)–N(1)	173.78(7)
K(1)–O(8)$^{\#3}$	2.7941(16)	O(9)–Co(1)–O(7)	177.73(7)
2			
Ni(1)–O(1)	2.0049(16)	K(1)–O(11)	2.8214(18)
Ni(1)–O(7)	2.0066(16)	K(1)–O(6)$^{\#3}$	2.8323(17)
Ni(1)–O(5)	2.0339(15)	K(1)–O(5)$^{\#3}$	2.8832(15)
Ni(1)–O(10)	2.0465(16)	K(1)–O(1)	2.9077(17)
Ni(1)–O(9)	2.0519(17)	K(1)–O(10)	2.9125(18)
Ni(1)–N(1)	2.1069(18)	K(1)–O(8)$^{\#1}$	3.0296(17)
Ni(1)–K(1)	3.5796(8)	K(1)–O(9)	3.068(2)
K(1)–O(7)$^{\#1}$	2.7455(17)	K(1)–O(11)$^{\#4}$	3.2117(19)
K(1)–O(6)$^{\#2}$	2.7553(17)	O(5)–Ni(1)–O(9)	178.18(7)
O(1)–Ni(1)–O(7)	172.99(6)	O(10)–Ni(1)–N(1)	175.42(7)

Symmetry codes for **1**: $^{\#1}-x+1/2,-y+1/2,-z+1$; $^{\#2}-x+1/2,y+1/2,-z+3/2$; $^{\#3}-x+1/2,-y+3/2,-z+1$, $^{\#4}-x+1/2,y-1/2,-z+3/2$. Symmetry codes for **2**: $^{\#1}x, -y, z-1/2$; $^{\#2}x, y-1, z$; $^{\#3}-x+1/2, -y+1/2, -z+1$; $^{\#4}-x+1/2, y+1/2, -z+1/2$.

The factors responsible for the template role of K^+ rather than Na^+ ions may be the hydration capacity of K^+ being weaker than Na^+ and the weaker polarization and stronger deformation ability [11b]. Homometallic complexes **3** and **4** were generated when KOH or 2,2′-bipyridine was substituted by NaOH or $NaHCO_3$, whether $NaNO_3$ was added or not. The mixture $EtOH/H_2O$ was favorable for the generation of **3** and **4**, providing a slower evaporation rate and a better solubility than MeOH.

IR spectra of **1** and **2** show strong and broad stretching bands at 3408 cm^{-1} and 3414 cm^{-1}, respectively, attributed to the O–H stretch of bound water. Bands at 1675–1676 cm^{-1} indicate incomplete deprotonation of carboxylic group of H_4L. Characteristic bands of carboxylates are at 1598–1600 and 1449 cm^{-1} for asymmetric stretches and symmetric stretches [15], respectively. In IR spectra of **3** and **4**, broad bands at 3321 and 3295 cm^{-1} can be assigned to the formation of O–H $\cdots$ O–H bonds. The absence of bands at 1670–1700 cm^{-1} suggests complete deprotonation of carboxylic group of H_4L. Bands of carboxylates are at 1579 cm^{-1} and 1451 cm^{-1} for asymmetric and symmetric stretches, respectively.

3.2. *Structure descriptions*

X-ray crystallographic diffractions reveals that **1** (figures S1 and S2) and **2** are isomorphous, crystallizing in the monoclinic crystal system with a $C2/c$ space group. Important bond lengths and angles are listed in table 2. The following descriptions are based on **1**. As shown in figure 1, **1** contains one repeat unit $[K_2Co_2(HL)_2(H_2O)_6]$, composed of two K^+, two Co^{2+}, two HL^{3-}, and six coordinated water molecules. Each

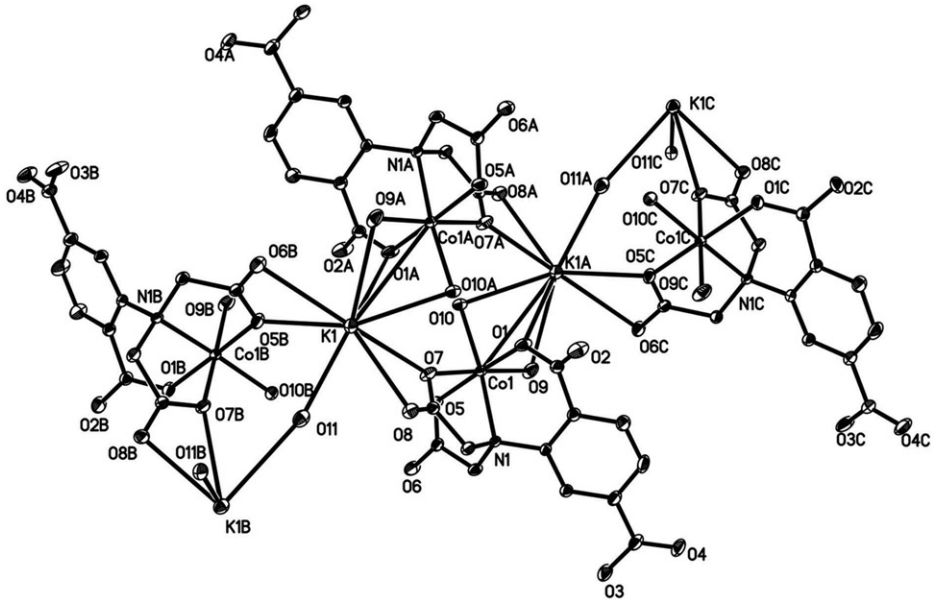

Figure 1. The diagram of **1** with numbering scheme.

symmetric Co^{2+} is located in an octahedral NO_5 geometry. The equatorial plane consists of one nitrogen (amino), two oxygen atoms (carboxyl), and one coordinated H_2O with an average Co–O distance of 2.040 Å. Axial positions are occupied by O7 (carboxyl) and O9 (H_2O) with mean bond distances of 2.076 Å to metal. Obviously, it is nearly an ideal octahedron. Each K^+ is coordinated by 10 oxygen atoms involving six carboxyl and four water molecules. The K–O distance is consistent with the reported values [16–20]. Neighboring Co^{2+} and K^+ ions are bridged by three μ_2-O from one carboxyl and two H_2O, and single μ_2-O atom (O7), resulting in a closed K_2Co_2 core. The K $\cdots$ Co distance is 3.620 Å. If the tetranuclear cores were considered as secondary building units, neighboring building units are linked by μ_2-O5 bridges between Co^{2+} and K^+, and by μ_2-O11 and double μ_2-O8 bridges between two K^+ ions. The Co $\cdots$ K and two K $\cdots$ K separations are 4.498, 6.017, and 4.086 Å, respectively. K^+ ions are set into a brick wall framework [21], with two Co^{2+} centers inserted in the middle of K_6 rectangles with Co $\cdots$ Co distance of 5.132 Å (figure 2); a 2-D layer framework is assembled. K^+ ions can be considered as templates in assembling 2-D layers.

In the 2-D layer, H_4L lost three protons and coordinates with one Co^{2+} and four K^+ ions as a hexadentate ligand. Three carboxylic groups exhibit various coordinated modes, 3.12, 2.21, and monodentate [22–25]. The free –COOH groups are distributed on both sides of the 2-D layer, forming interlayer H-bonds between O3 and O6 (carboxyl), and O4 and O9 (coordinated H_2O), respectively. H-bonds distances and angles are listed in table 3.

Isomorphous **3** (figure S3) and **4** are homometallic complexes and crystallize in monoclinic crystal systems with a $P2_1/n$ space group. Important bond lengths and angles are listed in table 4. The following description is based on **4**. As illustrated in figure 3, compound **4** is a dinuclear complex composed of one L^{4-}, two Ni^{2+}, and seven

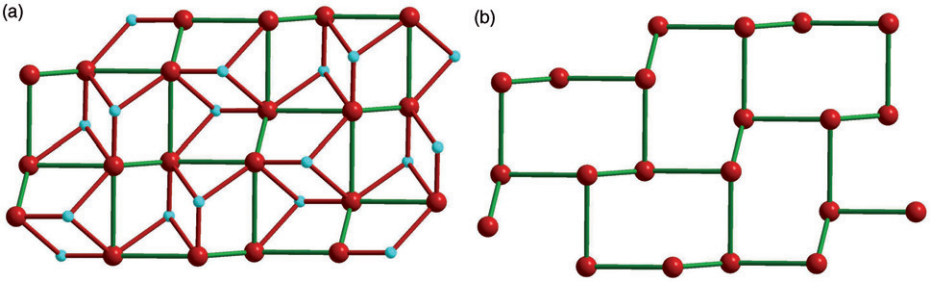

Figure 2. (a) The 2-D topology of **1**, K^+ and Co^{2+} ions are represented by dark red (large) and cyn (small) balls. The bridges linking K ··· K and K ··· Co are represented by green and dark red bonds; (b) the 2-D brick wall framework formed by K^+ ions (Color online).

Table 3. Important H-bond lengths (Å) and angles (°) of **3** and **4**.

D–H ··· A	*d*(D ··· A)	∠DHA	*d*(D–H)	Symmetry code of A
3				
O16–H23 ··· O8$^{\#1}$	2.886	167.31	0.883	$^{\#1}$ $-x+3/2, y+1/2, -z+1/2$
O17–H3 ··· O16$^{\#2}$	2.759	171.44	0.855	$^{\#2}$ $-x+3/2, y-1/2, -z+1/2$
O17–H21 ··· O8$^{\#2}$	2.856	169.28	0.841	
O15–H15 ··· O13$^{\#3}$	2.811	168.29	0.820	$^{\#3}$ $-x+1/2, y-1/2, -z+1/2$
O9–H1O4$^{\#4}$	2.661	174.39	0.786	$^{\#4}$ $-x+1, -y+2, -z$
4				
O17–H26 ··· O16	2.753	174.20	0.826	
O17–H27 ··· O6$^{\#1}$	2.833	169.82	0.809	$^{\#1}$ $-x+1/2, y-1/2, -z+1/2$
O16–H23 ··· O6$^{\#2}$	2.895	173.93	0.756	$^{\#2}$ $x, y-1, z$
O15–H15 ··· O12$^{\#3}$	2.806	162.45	0.820	$^{\#3}$ $-x-1/2, y+1/2, -z+1/2$
O10–H25 ··· O3$^{\#4}$	2.664	172.38	0.747	$^{\#4}$ $-x, -y+1, -z$

Table 4. Important bond lengths (Å) and angles (°) of **3** and **4**.

3			
Co(1)–O(10)	2.0327(14)	O(9)–Co(1)–O(5)	174.41(6)
Co(1)–O(1)	2.0376(14)	O(1)–Co(1)–O(7)	166.88(5)
Co(1)–O(5)	2.0714(13)	O(10)–Co(1)–N(1)	171.10(6)
Co(1)–O(7)	2.0869(14)	O(14)–Co(2)–O(11)	175.96(6)
Co(1)–N(1)	2.1893(16)	O(3)–Co(2)–O(15)	174.58(6)
Co(1)–O(9)	2.0400(14)	O(12)–Co(2)–O(13)	166.05(5)
4			
Ni(1)–O(10)	2.0046(19)	O(10)–Ni(1)–O(7)	175.82(8)
Ni(1)–O(1)	2.0111(19)	O(1)–Ni(1)–O(5)	171.83(7)
Ni(1)–O(9)	2.0155(18)	O(9)–Ni(1)–N(1)	171.92(8)
Ni(1)–O(7)	2.0292(17)	O(11)–Ni(2)–O(13)	175.69(8)
Ni(1)–O(5)	2.0533(19)	O(14)–Ni(2)–O(12)	167.52(8)
Ni(1)–N(1)	2.110(2)	O(4)–Ni(2)–O(15)	174.63(7)

coordinated water molecules. The coordination geometry around Ni1 is a slightly distorted octahedron. The Ni–N and average Ni–O distances in the equatorial plane composed of N1, O5, O9, and O1 are 2.110 and 2.026 Å, respectively. The axial positions are occupied by O7 and O10 with mean Ni–O distance of 2.011 Å,

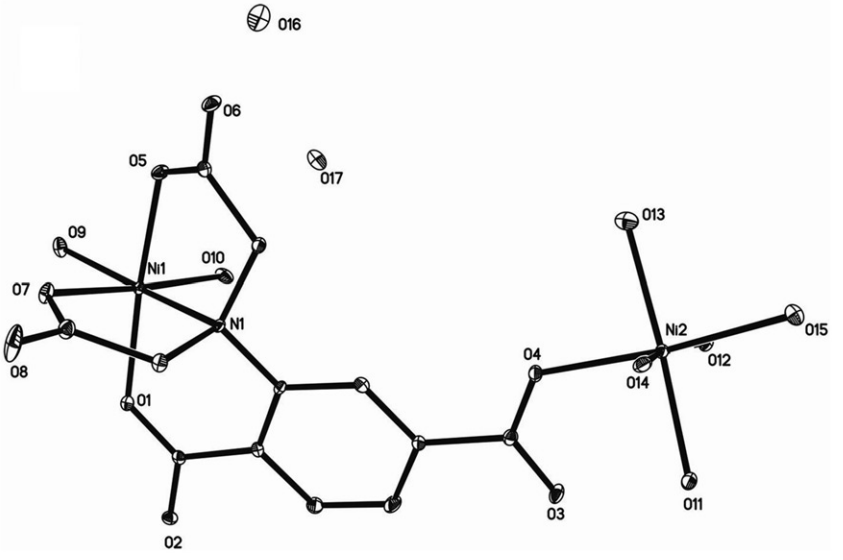

Figure 3. The ORTEP drawing of **4** with the thermal ellipsoids at the 30% probability.

respectively. Ni2 is located in a normal O_6 octahedral geometry composed of five H_2O and O4 of carboxyl. The average Ni–O distance in the equatorial plane formed by O4, O12, O15, and O14 is 2.082 Å. The axial sites are occupied by O11 and O13 with a Ni–O bond length of 2.045 Å. In **4**, L^{4-} is pentadentate coordinated with two metal ions. The Ni···Ni distance is 8.854 Å.

In **4**, two lattice H_2O play an important role in linking H-bond frameworks. As shown in figure 4(a), O16 and O17 have a role with O6 of two neighboring dinuclear molecules *via* O6···O16 and O6···O17, and also interact with each other by O16···O17 H-bond. Consequently, a right-hand H-bond helical chain O6···O16···O17··· is formed along the *b* direction. H-bond distances are 2.895, 2.752, and 2.834 Å, respectively. Adjacent Ni2 octahedra are linked by O12···O15 H-bonds, also resulting in left-hand helical chains along the *b*-axis (figure 4b). The H-bond length is 2.805 Å. Two helical chains combine to form a 2-D supramolecular framework. As exhibited in figure 4(c), O10 interacts with O3 *via* H-bonds, by which neighboring right-hand and left-hand helical chains connect in the *ac* plane. The O10···O3 bond length is 2.664 Å. As a result, a 3-D supramolecular framework illustrated as figure 4(d) is produced [26].

3.3. *Thermogravimetry (TG)*

To get information about thermal stability, $[K_4Co_4(HL)_4(H_2O)_{12}]$ (**1**), $[Co_2L(H_2O)_7]\cdot 2H_2O$ (**3**), and H_4L were studied by TG techniques from 298 K to 973 K and 298 K to 1073 K under nitrogen.

The TG chart of **1** exhibits three mass loss stages, starting at 380–440 K with the 8.15% mass loss, which corresponds to the loss of two water molecules (Calcd 8.06%).

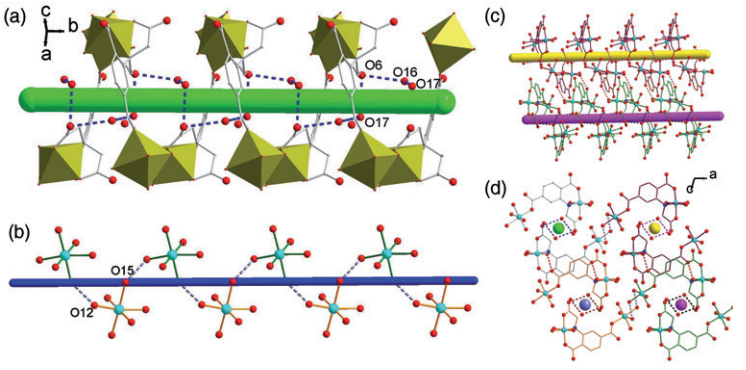

Figure 4. (a) 1-D H-bonds helical chain formed by O6, O16, O17 and labeled with blue dotted lines; (b) 1-D H-bond helical chain generated by Ni2 octahedra *via* H-bonds labeled with pale blue dotted lines; (c) 2-D layer structure linked by left-hand and right-hand helical chains *via* red dotted line H-bonds; and (d) 3-D supramolecular framework comprised of 2-D layer linked by Ni2 helical chains (Color online).

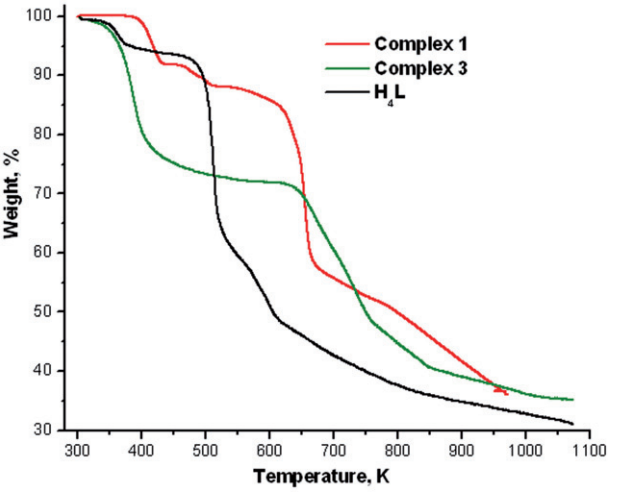

Figure 5. The TG curve of **1** from 298 to 973 K, **3** and H_4L from 298 to 1073 K.

The two H_2O should be the coordinated water molecules with long K–O bond distances (2.822 and 3.212 Å). On increasing temperature from 450 K, weight loss continues to 520 K. The weight loss in this step is 3.81%, assigned to the loss of one H_2O (Calcd 4.03%). The complex experiences a rapid loss at 650 K, which indicates the decomposition of HL^{3-}.

Two weight loss steps were observed in the TG curve of **3**. The first is from 310 K to 598 K with 28.20% mass loss, consistent with the loss of nine water molecules (Calcd 28.27%). From 598 K, the complex loses weight rapidly, and then experienced a slow mass loss from 855 to 1035 K with the sum value of 36.42%, from the decomposition of HL^{3-}.

H_4L experienced two main weight loses (figure 5). The first occurs at 320–420 K (6.13%), which can be considered as one H_2O from the transformation of two acetic

acids to acetic anhydride. As the temperature increased from 420 K, the skeleton of H_4L was damaged.

4. Conclusions

Four complexes containing cobalt(II) and nickel(II) were synthesized using H_4L. Extra K^+ in methanol is necessary for building the heterometallic 2-D layer coordination polymers **1** and **2**. Homometallic complexes **3** and **4** were obtained if K^+ ions were absent. Obviously, K^+ functions as a template and Na^+ cannot. In **3** and **4**, various H-bond helical chains were formed and extended to 3-D supramolecular frameworks. Thermal analysis shows that the stability order is **1** > **3** > H_4L.

Supplementary material

Crystallographic data and bond length and angles in CIF format for this article have been deposited in the Cambridge Crystallographic Data Centre. Copies of the data can be obtained free of charge on quoting the CCDC nos. 666930 (**1**), 658564 (**2**), 764418 (**3**), and 705837 (**4**) *via* www.ccdc.cam.ac.uk/conts/retrieving.html (or from the Cambridge Crystallographic Data Centre, 12 Union Road, Cambridge CB2 1EZ, UK; Fax: (+44) 1223-336033, E-mail: deposit@ccdc.cam.ac.uk).

Acknowledgments

This work was supported financially by the National Natural Science Foundation of China (20671018 and 21001078), Specialized Research Fund for the Doctoral Program of Higher Education (No. 200800561137), and the Open Project of Key Lab Adv Energy Mat Chem (Nankai Univ) (KLAEMC-OP201101).

References

[1] (a) P. Day. *Coord. Chem. Rev.*, **192**, 827 (1999); (b) B. Rather, B. Moulton, R.D.B. Walsh, M.J. Zaworotko. *Chem. Commun.*, 694 (2002); (c) C. Janiak. *Dalton Trans.*, **2781** (2003).
[2] (a) Y.Q. Huang, B. Ding, H.B. Song, B. Zhao, P. Ren, P. Cheng, H.G. Wang, D.Z. Liao, S.P. Yan. *Chem. Commun.*, 4906 (2006); (b) P. Ren, M.L. Liu, J. Zhang, W. Shi, P. Cheng, D.Z. Liao, S.P. Yan. *Dalton Trans.*, 4711 (2008).
[3] R. Feng, F.L. Jiang, M.Y. Wu, L. Chen, C.F. Yan, M.C. Hong. *Cryst. Growth Des.*, **10**, 2306 (2010).
[4] D.P. Li, X.H. Zhou, X.Q. Liang, C.H. Li, C. Chen, J. Liu, X.Z. You. *Cryst. Growth Des.*, **10**, 2136 (2010).
[5] (a) M. Orendáčc, L. Sedláková, E. Čižmár, A. Orendáčová, A. Feher. *Phys. Rev.*, **B81**, 214410 (2010); (b) V. Tangoulis, C.P. Raptopoulou, V. Psycharis, A. Terzis, K. Skorda, S.P. Perlepes, O. Cador, O. Kahn. *Inorg. Chem.*, **39**, 2522 (2000).
[6] (a) P. Mahata, D. Sarma, S. Matarajan. *J. Chem. Sci.*, **122**, 19 (2010); (b) R. Gheorghe, P. Cucos, M. Andruh, J.P. Costes, B. Donnadieu, S. Shova. *Chem. Eur. J.*, **12**, 187 (2006).

[7] (a) Q.K. Liu, J.P. Ma, Y.B. Dong. *J. Am. Chem. Soc.*, **132**, 7005 (2010); (b) K.L. Gurunatha, G. Mostafa, D. Ghoshal, T.K. Maji. *Cryst. Growth Des.*, **10**, 2483 (2010).
[8] M.L. Liu, W. Shi, H.B. Song, P. Cheng, D.Z. Liao, S.P. Yan. *CrystEngComm*, **11**, 102 (2009).
[9] H. Adams, R. Bastida, D.E. Fenton, B.E. Mann, L. Valencia. *Eur. J. Org. Chem.*, **8**, 1843 (1999).
[10] S.T. Guo, W.W. Wang, L.D. Deng, J.F. Xing, A.J. Dong. *Macromol. Chem. Phys.*, **211**, 1572 (2010).
[11] (a) J.X. Liu, R.L. Lin, L.S. Long, R.B. Huang, L.S. Zheng. *Inorg. Chem. Commun.*, **11**, 1085 (2008); (b) K.E. Laidig, P. Speers, A. Streitwieser. *Coord. Chem. Rev.*, **197**, 125 (2000).
[12] Y.O. Xu, D.Q. Yuan, B.L. Wu, L. Han, M.Y. Wu, F.L. Jiang, M.C. Hong. *Cryst. Growth Des.*, **5**, 1168 (2006).
[13] O.S. Jung, Y.J. Kim, Y.A. Lee, J.K. Park, H.K. Chae. *J. Am. Chem. Soc.*, **122**, 9921 (2000).
[14] Y.B. Dong, Y.Y. Jiang, J. Li, J.P. Ma, F.L. Liu, B. Tang, R.Q. Huang, S.R. Batten. *J. Am. Chem. Soc.*, **129**, 4520 (2007).
[15] D. Dobrzyjska, L.B. Jerzykiewicz, M. Duczmal. *Polyhedron*, **24**, 407 (2005).
[16] Y.P. Cai, C.Y. Su, A.W. Xu, B.S. Kang, Y.X. Tong, H.Q. Liu, S. Jie. *Polyhedron*, **20**, 657 (2001).
[17] M. Albrecht, O. Blau, R. Frohlich. *Chem. Eur. J.*, **5**, 48 (1999).
[18] M. Murrie, S. Parsons, R.E.P. Winpenny. *J. Chem. Soc., Dalton Trans.*, 1423 (1998).
[19] G.M. Yang, H.Z. Kou, D.Z. Liao. *Hua Xue Xue Bao (Acta Chim Sinica)*, **57**, 918 (1999).
[20] H. Miyasaka, N. Matsumoto, N.R.E. Gallo, C. Floriani. *Inorg. Chem.*, **36**, 670 (1997).
[21] (a) X.F. Zheng, L.G. Zhu. *Cryst. Growth Des.*, **9**, 4407 (2009); (b) X.Y. Wang, S.C. Sevov. *Chem. Mater.*, **19**, 4906 (2007).
[22] D. Coucouvanis, R.A. Reynolds III, W.R. Dunham. *J. Am. Chem. Soc.*, **117**, 7570 (1995).
[23] R.W. Saalfrank, I. Bernt. *Curr. Opin. Solid State Mater. Sci.*, **3**, 407 (1998).
[24] E.K. Brechin, O. Cador, A. Caneschi, C. Cadion, S.G. Harris, S. Parson, M. Vonci, R.E.P. Winpenny. *Chem. Commun.*, 1860 (2002).
[25] R.A. Coxall, S.G. Harris, D.K. Henderson, S. Parsons, P.A. Tasker, R.E.P. Winpenny. *J. Chem. Soc., Dalton Trans.*, 2349 (2000).
[26] C.A. Johnson II, O.B. Berryman, A.C. Sather, L.N. Zakhorov, M.M. Haley, D.W. Johnson. *Cryst. Growth Des.*, **9**, 4247 (2009).